

University of Groningen

Intestinal de novo phosphatidylcholine synthesis is required for dietary lipid absorption and metabolic homeostasis

Kennelly, John P; van der Veen, Jelske N; Nelson, Randal C; Leonard, Kelly-Ann; Havinga, Rick; Buteau, Jean; Kuipers, Folkert; Jacobs, Rene L

Published in:
Journal of Lipid Research

DOI:
[10.1194/jlr.M087056](https://doi.org/10.1194/jlr.M087056)

IMPORTANT NOTE: You are advised to consult the publisher's version (publisher's PDF) if you wish to cite from it. Please check the document version below.

Document Version
Publisher's PDF, also known as Version of record

Publication date:
2018

[Link to publication in University of Groningen/UMCG research database](#)

Citation for published version (APA):

Kennelly, J. P., van der Veen, J. N., Nelson, R. C., Leonard, K-A., Havinga, R., Buteau, J., Kuipers, F., & Jacobs, R. L. (2018). Intestinal de novo phosphatidylcholine synthesis is required for dietary lipid absorption and metabolic homeostasis. *Journal of Lipid Research*, 59(9), 1695-1708.
<https://doi.org/10.1194/jlr.M087056>

Copyright

Other than for strictly personal use, it is not permitted to download or to forward/distribute the text or part of it without the consent of the author(s) and/or copyright holder(s), unless the work is under an open content license (like Creative Commons).

The publication may also be distributed here under the terms of Article 25fa of the Dutch Copyright Act, indicated by the "Taverne" license. More information can be found on the University of Groningen website: <https://www.rug.nl/library/open-access/self-archiving-pure/taverne-amendment>.

Take-down policy

If you believe that this document breaches copyright please contact us providing details, and we will remove access to the work immediately and investigate your claim.

Downloaded from the University of Groningen/UMCG research database (Pure): <http://www.rug.nl/research/portal>. For technical reasons the number of authors shown on this cover page is limited to 10 maximum.

Intestinal *De Novo* Phosphatidylcholine Synthesis is Required for Dietary Lipid Absorption and
Metabolic Homeostasis

John P. Kennelly^{1,2}, Jelske N. van der Veen^{1,3}, Randal C. Nelson¹, Kelly-Ann Leonard^{1,2}, Rick
Havinga⁴, Jean Buteau², Folkert Kuipers⁴, René L. Jacobs^{1,2,3,*}

¹ Group on the Molecular and Cell Biology of Lipids, University of Alberta, Edmonton, Canada;

² Department of Agricultural, Food and Nutritional Science, University of Alberta, Edmonton,
Canada;

³ Department of Biochemistry, University of Alberta, Edmonton, Canada;

⁴ Departments of Pediatrics and Laboratory Medicine, University of Groningen, University
Medical Center Groningen, Groningen, The Netherlands

* Corresponding author. Email: rjacobs@ualberta.ca. Mailing address: 4-002E Li Ka Shing
Centre for Health Research and Innovation, University of Alberta, T6G2E1, AB, Canada. Phone:
+1-780-492-2343. Fax: +1-780-492-2343.

Running title: Phosphatidylcholine synthesis controls intestinal function.

Abbreviations: CT, CTP:phosphocholine cytidyltransferase; FGF21, Fibroblast-like growth
factor 21; GLP-1, glucagon-like peptide 1; H&E, hematoxylin and eosin; HFD, high fat diet;
FPLC, fast protein liquid chromatography; PC, phosphatidylcholine; PE,
phosphatidylethanolamine; PYY, peptide YY; TG, triglyceride.

ABSTRACT

De novo phosphatidylcholine (PC) synthesis via CTP:phosphocholine cytidylyltransferase- α (CT α) is required for very-low-density lipoprotein secretion. To determine the precise role of *de novo* PC synthesis in intestinal lipid metabolism, we deleted CT α exclusively in the intestinal epithelium of mice (CT α^{IKO} mice). When fed a chow diet, CT α^{IKO} mice showed normal fat absorption despite a ~30% decrease in intestinal PC concentrations relative to control mice, suggesting that biliary PC can fully support chylomicron secretion under these conditions. However, when fed a high-fat diet, CT α^{IKO} mice showed impaired passage of fatty acids and cholesterol from the intestinal lumen into enterocytes. Impaired intestinal lipid uptake in CT α^{IKO} mice was associated with lower plasma triglyceride concentrations, higher plasma Glucagon-like Peptide 1 and Peptide YY, and disruption of intestinal membrane lipid transporters after a high fat meal relative to control mice. Unexpectedly, biliary bile acid and PC secretion was enhanced in CT α^{IKO} mice due to a shift in expression of bile-acid transporters to the proximal intestine, indicative of accelerated enterohepatic cycling. These data show that intestinal *de novo* PC synthesis is required for dietary lipid absorption during high-fat feeding and that the re-acylation of biliary lyso-PC cannot compensate for loss of CT α under these conditions.

Keywords: Absorption, bile, phospholipids, lipids and lipoprotein metabolism, chylomicrons, triglycerides, intestine, GLP-1, PYY.

INTRODUCTION

Phospholipids form the matrix of biological membranes, provide precursors for a variety of signaling molecules, and allow assembly and secretion of lipoproteins (1).

Phosphatidylcholine (PC) is the primary phospholipid in eukaryotic cells (1). The amphitropic enzyme CTP: phosphocholine cytidylyltransferase (CT) regulates *de novo* PC synthesis in response to changes in membrane lipid composition in all nucleated mammalian cells (2). Global deletion of CT α (encoded by *Pcytl1a*) is embryonic lethal in mice, reflecting the essential role of membrane biogenesis during development (3). Mice lacking CT α in the liver have impaired very-low-density lipoprotein (VLDL) secretion and accumulate neutral lipids in hepatocytes (4) despite the presence of a second route for hepatic PC synthesis *via* the methylation of phosphatidylethanolamine (PE) by phosphatidylethanolamine-N-methyltransferase (PEMT). Similarly, CT α cannot compensate for the loss of PEMT in generating PC for VLDL assembly (5).

Intestinal PC can be derived from the diet, bile, circulating lipoproteins, and from local *de novo* synthesis. Dietary and biliary PC is hydrolyzed in the intestinal lumen by phospholipase A2 to lyso-PC and fatty acids before being absorbed into enterocytes, delivered to the endoplasmic reticulum, and re-acylated into PC by lyso-PC acyltransferase (Lpcat) enzymes (6, 7). Mice lacking hepatic Abcb4, which is required for PC secretion into bile, have normal passage of fatty acids from the intestinal lumen into enterocytes but have impaired chylomicron assembly and secretion, highlighting the importance of biliary PC for chylomicron output (8). Furthermore, loss of intestinal Lpcat3, which incorporates polyunsaturated fatty acids into PC, impairs dietary lipid absorption despite maintenance of total intestinal PC mass (9, 10). Conversely, increasing the delivery of PC to the intestinal lumen promotes chylomicron

secretion (11). Therefore, while the re-acylation of lyso-PC derived from the intestinal lumen is important for chylomicron production, the precise contribution that intestinal *de novo* PC synthesis makes to this process is unknown.

In the present study we hypothesized that loss of intestinal CT α activity would cause TG accumulation in enterocytes due to insufficient supply of PC for chylomicron assembly. However, we unexpectedly found that loss of intestinal *de novo* PC synthesis impairs passage of fatty acids from the intestinal lumen into enterocytes in the setting of a high fat diet (HFD), but not a chow diet. Fat malabsorption is linked to the repression of genes involved in fatty acid uptake, enhanced postprandial enteroendocrine hormone secretion, and reduced adiposity. Furthermore, we show that loss of intestinal CT α promotes biliary bile acid and lipid secretion by accelerating enterohepatic bile acid cycling. Our data provide evidence of a specific requirement for intestinal *de novo* PC synthesis in the maintenance of intestinal metabolic functions and show that the re-acylation of lyso-PC from extra-intestinal sources is insufficient to maintain metabolic function during HFD feeding.

MATERIALS AND METHODS

Generation of mice with intestine-specific deletion of *Pcyt1a*

Mice carrying a floxed *Pcyt1a* locus (*Pcyt1a*^{LoxP/LoxP}) on a C57BL/6J background were crossed with mice expressing a tamoxifen-inducible Cre-recombinase transgene under the control of a villin promoter (villin-CreER^{T2}) (12) to generate *Pcyt1a*^{LoxP/WT};villin-CreER^{T2} mice (with the capacity to induce a heterozygous deletion of intestinal CT α after tamoxifen treatment).

Subsequent cross-breeding of *Pcyt1a*^{LoxP/WT};villin-CreER^{T2} mice resulted in the generation of

Pcytl1a^{LoxP/LoxP};villin-CreER^{T2} mice (with the capacity to induce a homozygous deletion of intestinal CTα after tamoxifen treatment). Genomic DNA was extracted from tail biopsies with a DNeasy Blood and Tissue Kit (Qiagen, UK). PCR products were identified on a 3% agarose gel (floxed *Pcytl1a* band) or a 1.5% agarose gel (Villin Cre-inducible band). Cre was induced in 8-12-week-old male or female mice by intraperitoneal injection of tamoxifen (1mg/day in sunflower oil for 5 days; Sigma, St. Louis, MO), while tamoxifen-treated *Pcytl1a*^{LoxP/LoxP} mice were used as controls. Mice were fed a chow diet (5001, Lab Diet, St. Louis, MO) or a semi-purified HFD containing 40% kilocalories as fat (Supplementary Table S1). Mice were housed in a temperature-controlled room with 12-h light/dark cycle and free access to food and water. Samples were collected after a 10-h fast or after overnight fasting followed by 2-h re-feeding, unless otherwise stated. Small intestines were excised, flushed with phosphate buffered saline (PBS) containing protease inhibitor cocktail (Sigma, St. Louis, MO), and kept on ice. The small intestine was divided into 3 portions of length ratio 1:3:2 (corresponding to duodenum: jejunum: ileum) before jejunum sections were fixed in 10% neutral-buffered formalin for histology. Epithelial cells were collected in liquid nitrogen after segments were opened longitudinally. The University of Alberta's Institutional Animal Care Committee approved all animal procedures, which were in accordance with guidelines of the Canadian Council on Animal Care.

Microscopy

Formalin-fixed, paraffin-embedded tissue slices (5μm thick) were stained with hematoxylin and eosin (H&E) and visualized with a light microscope. For electron microscopy, 2cm jejunal rings were fixed with 2% paraformaldehyde and 2.5% glutaraldehyde in 0.1M phosphate buffer (pH 7.2). Sections were cryo-sectioned with an ultramicrotome (Ultracut E, Reichert-Jung) equipped

with an FC4D attachment, and images were obtained using a Philips 410 transmission electron microscope.

mRNA isolation and quantification by PCR

Total RNA was isolated from intestinal scrapings or liver using Trizol (Invitrogen, CA, USA). RNA was reversed-transcribed using Superscript II (Invitrogen, CA, USA). Quantitative PCR was run on an Applied Biosystems StepOne Plus for 40 cycles using a Power SYBR Green PCR Master Mix (Applied Biosystems, MA, USA), in triplicate. Relative mRNA expression was normalized to cyclophilin. Quantitation was performed using the standard curves method. Primer sequences are listed in Supplementary Table S2.

Fatty acid absorption

Intestinal fatty acid absorption was quantified as described previously (13), with modifications. Briefly, male control and $CT\alpha^{IKO}$ mice were fasted for 4 h before receiving an oral gavage of 150 μ L of olive oil containing 5 μ Ci [3 H]-labelled triolein. Blood was collected at 30, 60, 90 and 120 mins post-gavage. At 120 mins post-gavage, the small intestine was excised, flushed with 40ml PBS containing 0.5mM sodium taurocholate and cut into 2cm segments. Segments were dissolved in 1N NaOH for 3 days at 60°C. Plasma and tissue [3 H]-label was measured by liquid scintillation counting (Beckman Coulter Inc, CA). For poloxamer studies, mice were fasted for 10 h before receiving an intraperitoneal injection of Poloxamer-407 (1g/kg; Sigma, MO, USA) and an oral gavage of 150 μ L olive oil. Blood was collected before, and every hour for 4 h after the oil challenge. Plasma TG concentrations were assessed using a commercially available kit (Sekisui Diagnostics, MA). To visualize intestinal lipid droplets after a fat challenge, 4-h fasted female mice were gavaged (7.5 μ L/g mouse) with olive oil containing 20% Bodipy 500/510 C1,

C12 (D3823, Invitrogen, CA, USA). Sections of the proximal small intestine were embedded in optimum cutting temperature (OCT) and sliced on cryostat at -20 degrees Celsius. Slides were mounted with Prolong Diamond Antifade Mountant containing DAPI (P36962, Invitrogen, CA, USA) before images were obtained with a fluorescence microscope (Olympus, Markham, ON) equipped with Suveyor and ImagePro Plus software.

Cholesterol absorption

Individually-housed male control and $CT\alpha^{IKO}$ mice received an oral dose of [3H]-cholesterol (2 μ Ci) with 6mg unlabeled cholesterol in 150 μ L of olive oil, and an intravenous injection of [^{14}C]-cholesterol (1 μ Ci) mixed in Intralipid[®]. Blood and feces was collected at 24, 48 and 72 h after cholesterol administration. Blood was centrifuged at 3000g for 10 minutes and plasma was collected. Plasma [3H]-label and [^{14}C]-label was measured by liquid scintillation counting (Beckman Coulter Inc, CA). The [3H]-label and [^{14}C]-label in fecal neutral sterol and fecal bile salt (aqueous) fractions were measured by liquid scintillation counting (Beckman Coulter Inc, CA) after separation of the fractions by the method of Folch (14).

Gallbladder cannulations and bile measurements

For gallbladder cannulations, male mice were anesthetized by intraperitoneal injection of ketamine (100mg/kg)/ xylazine (10mg/kg). Gallbladders were cannulated with silastic tubing (Dow Corning, MI; internal diameter 0.5mm) after ligation of the common bile duct beside the duodenum. Mice were placed in a humidified incubator and bile was collected for 30 mins in pre-weighed vials. Bile acid species composition (including taurohyodeoxycholic acid (THDCA), tauro- β -muricholic acid (TB-MCA), tauro- α -muricholic acid (TA-MCA), β -muricholic acid (β -MCA), taurodeoxycholic acid (TDCA), taurochenodeoxycholic acid

(TCDCA), taurocholic acid (TCA), tauroursodeoxycholic acid (TUDCA) and cholic acid (CA)) was determined by liquid chromatography tandem mass spectrometry (LC-MS/MS) as described previously (15). The hydrophobicity of bile acids was determined according to the method of Heuman (16). Biliary lipids were extracted by the method of Folch (14). Biliary phospholipid concentrations were assessed by phosphorous assay, as described previously (17). Biliary cholesterol concentrations were measured with a commercially available kit (WAKO Chemicals, USA). Biliary secretion rates were calculated by multiplying biliary bile acid, phospholipid, or cholesterol concentrations by bile flow ($\mu\text{L}/\text{min}$). Bile acid concentrations in feces and plasma were determined by enzymatic fluorometric assay (18).

Plasma, tissue, and fecal lipid analysis

Plasma TG (Sekisui Diagnostics, MA, USA), cholesterol (Wako Chemicals, USA) and non-esterified fatty acids (Wako Chemicals, USA) were measured with commercially available kits. Lipoprotein fractions were separated from pooled plasma samples (5 mice per group) by size exclusion fast protein liquid chromatography (FPLC) before measuring TG and cholesterol concentrations by commercially-available kits (Lipidomics Core Facility, University of Alberta). Total protein concentrations of tissue homogenates were determined by bicinchoninic acid assay before tissue lipids were extracted from homogenates (1mg/ml) by the method of Folch (14). PC and phosphatidylethanolamine (PE) were separated by thin layer chromatography using the solvent system chloroform:methanol:acetic acid:water (50:30:8:4). Bands were visualized after exposure to iodine and measured by phosphorous assay, as described previously (17). Intestinal TG concentrations were measured using a commercially available kit (Sekisui Diagnostics, MA, USA). The relative abundance of PC species in jejunal epithelial cells was measured by mass spectrometry at The Metabolomics Innovation Centre, University of Alberta. To analyze the fatty

acid composition of intestinal PC, lipids were extracted from intestinal scrapings and separated by thin-layer chromatography as described above. PC bands were recovered from the plates and converted to fatty acid methyl esters by incubation with 2 ml of hexane (Sigma Aldrich, 293253) and 1.5ml boron trifluoride (Sigma-Aldrich, B1252) in methanol for 1 h at 110 °C. Fatty acid methyl esters were then analyzed by gas-liquid chromatography (results are shown as the percentage of total fatty acids measured). Intestinal non-esterified cholesterol and cholesterol esters were measured by gas-liquid chromatography with flame ionization detection (GC-FID) after derivatization with bis(trimethylsilyl)trifluoroacetamide and adjustment of peaks with the internal standard tridecanoin, as described previously (19). Fecal samples (50mg) were dried and ground to a powder before extraction of lipids by the method of Folch (14). Non-esterified fatty acid and cholesterol concentrations in feces of female mice collected over 72 h were determined with commercially available kits (Wako Chemicals, USA).

Measurement of intestinal CT activity

Intestinal CT α activity was determined by measuring the conversion of [3 H]phosphocholine into [3 H]CDP-choline, as described previously (4).

Plasma metabolite measurements

Blood glucose was measured from the tail vein with a glucometer (Accu-chek, Roche, Switzerland) after a 10-h fast, after 2 h re-feeding or after 2 h re-feeding followed by an oral gavage of glucose (2mg/g body weight). Blood was collected by cardiac puncture in tubes containing EDTA, dipeptidyl peptidase 4 inhibitor (EMD Millipore, MA, USA) and Complete[®] general protease inhibitor (Sigma, MO, USA) before being centrifuged at 3000g for 10 minutes to obtain plasma. Plasma insulin (Meso Scale Diagnostics, MD, USA), leptin (Meso Scale

Diagnostics, MD, USA), active GLP-1 (EMD Millipore, MA, USA), PYY (Crystal Chem IL, USA), and FGF21 (Abcam, Cambridge, UK) were measured by enzyme-linked immunosorbent assay, according to the manufacturer's instructions. Plasma (4 μ L) was resolved on a sodium dodecyl sulfate polyacrylamide gel (5% gel for ApoB and 10% for ApoA1). Proteins were transferred to a polyvinylidene difluoride membrane and probed with either anti-Apolipoprotein B (dilution 1:7500, AB742; Chemicon, MA, USA) or Anti-Apolipoprotein A1 (dilution 1:2000; K23001R, BioDesign/Meridian). ApoB and ApoA1 were run on separate gels. Immunoreactive proteins were detected with Enhanced ChemiLuminescence (ECL; Amersham, GE Healthcare, UK), and blots were imaged with a ChemiDoc MP Imager, (Bio-rad Laboratories, CA, USA).

Statistics

Data are expressed as mean \pm standard error of the mean using Graphpad Prism 7 (GraphPad Software, La Jolla, CA); $p < 0.05$ was considered statistically significant. Student's t-test was used to compare two independent groups. A one-way ANOVA was used when comparing 3 groups with one experimental outcome. A two-way ANOVA with Bonferroni post-test was used to determine the effect of genotype and time on an experimental outcome.

RESULTS

Intestinal PC concentrations are reduced in CT α ^{IKO} mice fed a chow diet, but fat absorption capacity is unaltered.

Induction of Cre recombinase with tamoxifen in *Pcytl α* ^{LoxP/LoxP};villin-CreER^{T2} mice (herein referred to as CT α ^{IKO} mice) reduced *Pcytl α* mRNA abundance and CT α enzyme activity in the

jejunum and ileum by >90% compared to tamoxifen-treated *Pcytl*^{LoxP/LoxP} control mice (Fig. 1A and 1B and supplementary Fig. S1A). *Pcytl* mRNA remained repressed in the intestines of CT α ^{IKO} mice for at least 50 days following Cre induction (supplementary Fig. S1B). Characterization of mice with a heterozygous deletion of intestinal CT α fed either a chow diet (supplementary Fig. S1D-S1H) or a HFD (supplementary Fig. S1I-S1M) revealed no differences in body weight, blood glucose, plasma lipids, or fat absorption after an oral lipid bolus despite a ~50% decrease in intestinal *Pcytl* mRNA abundance compared to control mice (supplementary Fig. S1C).

Loss of intestinal CT α did not impact survival of the mice fed the chow diet, and body mass of CT α ^{IKO} mice was comparable to that of controls after 6 weeks (Fig. 1C). Furthermore, histological examination of H&E-stained jejunum sections at 6 weeks after Cre induction revealed no overt morphological abnormalities in CT α ^{IKO} intestines compared to control intestines (Fig. 1D). This finding suggests that intestinal CT α activity is not required for maintenance of epithelial cell turnover in adult mice. PC concentrations were lower in the jejunum and ileum of CT α ^{IKO} mice compared to controls after an oil challenge (Fig. 1E). Furthermore, PE concentrations were higher in the jejunum of CT α ^{IKO} mice (Fig. 1F). This resulted in a relatively large decrease in the molar ratio of PC-to-PE in the intestines of CT α ^{IKO} mice (Fig. 1G). Fasting plasma cholesterol concentrations (Fig. 1H) were significantly lower in CT α ^{IKO} mice fed the chow diet, while fasting plasma TG (Fig. 1I), insulin and blood glucose concentrations (not shown) were unchanged compared to control mice.

Unexpectedly, despite the absence of intestinal CT α activity and a dramatic decrease in the PC/PE ratio of intestinal membranes, TG appearance in plasma was comparable between CT α ^{IKO} mice and control mice after an oral bolus of olive oil (Fig. 1J). This finding suggests that, in

contrast to the liver where 'new' PC synthesis is required for VLDL secretion (4), intestinal *de novo* PC synthesis is dispensable for chylomicron secretion in the setting of a low-fat diet. These results also suggest that PC supplied to the intestine in bile is sufficient for chylomicron formation and secretion under these conditions.

HFD feeding initially induces rapid weight loss, while chronic HFD feeding reduces weight gain, in $CT\alpha^{IKO}$ mice

We hypothesized that feeding mice a HFD would increase demand for lipid droplet and chylomicron PC and therefore induce more pronounced changes to the intestinal epithelium of $CT\alpha^{IKO}$ mice. Analysis of 3 independent experiments showed that 26% of $CT\alpha^{IKO}$ mice (5 of 19) lost ~25% body weight and displayed steatorrhea between days 4 and 5 following initiation of the HFD, forcing termination of these mice under protocol requirements (Fig. 2A). Interestingly, the remaining 74% of $CT\alpha^{IKO}$ mice experienced only modest weight loss but had significantly less visceral fat mass and lower plasma leptin concentrations than did control mice on day 6 following initiation of the HFD (Fig. 2B and 2C). Weight loss in $CT\alpha^{IKO}$ mice coincided with reduced food intake ($2.76 \text{ g} \pm 0.25$ by control mice compared to $1.36 \text{ g} \pm 0.21$ by $CT\alpha^{IKO}$ mice between 48 and 72 h after initiation of the HFD, $P=0.0009$).

The $CT\alpha^{IKO}$ mice fed a HFD for 50 days gained 20% less body weight and had 40% less visceral fat mass compared to controls (Fig. 2D and 2E). The lower food intake observed in $CT\alpha^{IKO}$ mice compared to control mice in the first week following initiation of the HFD appeared to be an acute response to the diet, as food intake was similar between $CT\alpha^{IKO}$ mice and control mice by week 6 following HFD initiation ($2.257 \pm 0.16 \text{ g/day}$ for control mice compared to $2.034 \pm 0.17 \text{ g/day}$ for $CT\alpha^{IKO}$ mice, $P=0.36$). Nevertheless, fasting blood glucose was significantly lower in $CT\alpha^{IKO}$ mice (Fig. 2F). In contrast to liver-specific $CT\alpha$ knockout mice (4), fasting

plasma TG and cholesterol concentrations were not reduced in $CT\alpha^{IKO}$ mice after being fed a HFD for 6 days or 50 days (Fig. 2G and 2H). Taken together, these data show that HFD feeding induces weight loss, while chronic feeding reduces weight gain in $CT\alpha^{IKO}$ mice.

Loss of intestinal $CT\alpha$ reduces chylomicron lipidation during HFD feeding

To determine whether impaired dietary lipid absorption contributed to the acute weight loss in $CT\alpha^{IKO}$ mice fed the HFD, we assessed postprandial plasma lipid concentrations. Control and $CT\alpha^{IKO}$ mice were fasted overnight on day 3 following initiation of the HFD (prior to onset of severe weight loss) before re-feeding them for 2 h. Food intake was similar between $CT\alpha^{IKO}$ mice and control mice during HFD re-feeding (not shown). Plasma TG concentrations were 60% lower and plasma non-esterified fatty acid concentrations were 30% lower in $CT\alpha^{IKO}$ mice compared to controls after 2 h HFD re-feeding (Fig. 3A). Furthermore, $CT\alpha^{IKO}$ mice had markedly less TG in the largest lipoprotein fraction compared to controls (Fig. 3B). Interestingly, despite a dramatic difference in plasma TG concentrations between genotypes after re-feeding, plasma ApoB concentrations were not different (Fig. 3C). This finding strongly suggests that lipidation of the intestine-derived lipoprotein particles was impaired in $CT\alpha^{IKO}$ mice, whereas the number of particles secreted was not reduced. Total plasma cholesterol concentrations were similar between $CT\alpha^{IKO}$ mice and control mice after HFD re-feeding (Fig. 3A). However, $CT\alpha^{IKO}$ mice had less cholesterol in the largest lipoprotein fraction, while high-density lipoprotein (HDL) cholesterol (Fig. 3D) and plasma ApoA1 concentrations were not different between genotypes (Fig. 3C). To determine whether enhanced particle clearance contributed to the low postprandial plasma TG in $CT\alpha^{IKO}$ mice, we challenged the mice with an intra-gastric bolus of olive oil after intra-peritoneal injection of Poloxamer-407, an inhibitor of lipoprotein lipase. Intestinal TG secretion remained blunted in $CT\alpha^{IKO}$ mice over the 4 h study period (Fig.

3E). Lower plasma TG after re-feeding was also observed in $CT\alpha^{IKO}$ mice compared to controls fed a HFD for 6 weeks (1.14 ± 0.06 mmol/L in control mice compared to 0.83 ± 0.09 mmol/L in $CT\alpha^{IKO}$ mice, $P=0.03$). Taken together, these data show that the intestine secretes TG-poor ApoB-containing particles in the absence of *de novo* PC synthesis.

Loss of intestinal $CT\alpha$ impairs fatty acid uptake from the intestinal lumen into enterocytes

We hypothesized that impaired intestinal TG secretion in $CT\alpha^{IKO}$ mice was due to TG accumulation in enterocytes. However, $CT\alpha^{IKO}$ mice had significantly lower jejunal TG concentrations than control mice after fasting and re-feeding (Fig. 4A and 4B). To track the spatial distribution of fatty acid uptake in the small intestine, we gavaged mice with [3H]-labeled triolein. The radioactivity in the mid-intestine of $CT\alpha^{IKO}$ mice, where fatty acid absorption is typically highest, was strikingly lower than in control mice (Fig. 4C). As expected based on previous results, appearance of [3H]-label in plasma was significantly blunted in $CT\alpha^{IKO}$ mice (Fig. 4D). Taken together, these data indicate that loss of intestinal $CT\alpha$ impairs fatty acid uptake from the intestinal lumen into enterocytes in the setting of a HFD.

Histological examination of jejunal sections 2 h after a bolus of olive oil revealed fewer lipid droplets in enterocytes of $CT\alpha^{IKO}$ mice compared to control mice fed the HFD (Fig. 4E). We also detected markedly fewer fluorescent lipid droplets in enterocytes of $CT\alpha^{IKO}$ mice gavaged with Bodipy-labeled fatty acids (Fig. 4F). Moreover, electron microscopy showed a general absence of cytosolic lipid droplets in HFD-fed $CT\alpha^{IKO}$ enterocytes 2 h after an oil challenge (Fig. 4G). Consistent with lower fatty acid concentrations in enterocytes, the mRNA levels of *monoacylglycerol O-acyltransferase 2* (*Mogat2*), *diacylglycerol O-acyltransferase 2* (*Dgat2*) and lipid droplet-associated *abhydrolase domain containing 5* (*Abhd5*) and *cell death-inducing DFFA-like effector c* (*Cidec*) were significantly lower in $CT\alpha^{IKO}$ intestines 2 h after a

meal (Fig. 4H). These data suggest that impairment of intestinal PC synthesis reduces fatty acid uptake from the intestinal lumen and thereby limits fatty acid supply for lipid droplet and chylomicron formation. In further support of impaired fat absorption, non-esterified fatty acids were elevated in feces of CT α ^{IKO} mice compared to control mice (Fig. 4I).

Loss of intestinal CT α impairs intestinal cholesterol absorption

Cholesterol concentrations were also significantly higher in feces of CT α ^{IKO} mice compared to control mice (Fig. 5A). To examine cholesterol turnover, control and CT α ^{IKO} mice were administered with an oral gavage of [³H]-cholesterol and an intravenous injection of [¹⁴C]-cholesterol, and the labels were measured in plasma and feces over 72 h. After 24 h, the appearance of [³H]-cholesterol in the circulation of CT α ^{IKO} mice was significantly lower than in control mice (Fig. 5B). Furthermore, cumulative fecal excretion of [³H]-neutral sterols over 72 h was higher in CT α ^{IKO} mice (Fig. 5C). These data suggest that luminal cholesterol absorption is impaired with loss of intestinal CT α . The rate of disappearance of radiolabel from plasma after intravenous injection of [¹⁴C]-cholesterol and cumulative [¹⁴C] accumulation in fecal neutral sterols was not different between genotypes (Fig. 5D and 5E), suggesting that hepatic cholesterol uptake was unaltered by loss of intestinal CT α . Furthermore, there was no difference in appearance of [³H] or [¹⁴C] in fecal bile salts between genotypes, suggesting that hepatic bile acid synthesis was not changed in response to reduced intestinal cholesterol absorption in CT α ^{IKO} mice (Fig. 5F and 5G). Despite impaired cholesterol absorption, jejunal cholesterol and cholesterol ester concentrations were unchanged in CT α ^{IKO} mice relative to controls (Fig. 5H and 5I). Accordingly, mRNA abundance of several genes linked to cholesterol biosynthesis, including *mevalonate kinase (Mvk)*, *farnesyl diphosphate synthase (Fdps)*, *cytochrome P450, family 51 (Cyp51)* and *NAD(P) dependent steroid dehydrogenase-like (Nsdhl)*, were induced in

the jejunum of $CT\alpha^{IKO}$ mice relative to controls (Fig. 5J). Induction of intestinal cholesterol biosynthesis in $CT\alpha^{IKO}$ mice might be a compensatory response to impaired cholesterol absorption, or it might be due to altered intestinal phospholipid homeostasis in epithelial cells, as has recently been described (20).

Impaired lipid absorption in $CT\alpha^{IKO}$ mice is linked to reduced expression of plasma membrane lipid transporters

Microvillus length and structure were comparable between genotypes, suggesting that lipid malabsorption in $CT\alpha^{IKO}$ mice is not due to structural damage to the intestinal epithelium (Fig. 6A). Intestinal *Lpcat3* deletion in mice reduces passive lipid diffusion into enterocytes by reducing the incorporation of polyunsaturated fatty acids into intestinal PC (9, 10). The mRNA levels of *Lpcat3* were not altered in $CT\alpha^{IKO}$ mice relative to controls (Fig. 6B). As expected, jejunal PC concentrations were significantly lower in $CT\alpha^{IKO}$ mice re-fed the HFD, while PE concentrations were unchanged compared to controls (Fig. 6C and Fig 6D). However, the relative abundance of PC molecular species as measured by mass spectrometry was only minimally different between genotypes, with small increases in the relative abundance of PC (36:2) and PC (38:3) observed in $CT\alpha^{IKO}$ mice (Fig. 6E). To validate our mass spectrometry results we performed gas-liquid chromatography analysis of the acyl chain constituents of PC and confirmed that the composition of fatty acids acylated to PC in the proximal intestine was comparable between genotypes (Fig. 6F). Therefore, impaired lipid absorption in $CT\alpha^{IKO}$ mice is not due to changes in the relative abundance of PC molecular species as observed in mice deficient in intestinal *Lpcat3*. However, altered PC/PE ratio of intestinal membranes may impair passive lipid diffusion into enterocytes of $CT\alpha^{IKO}$ mice.

The membrane lipid transporters *Cluster-determinant 36 (Cd36)*, *Solute Carrier Family 27 Member 4 (Slc27a4; Fatty acid transport protein 4)* and *NPC1 like intracellular cholesterol transporter 1 (Npc1l1)* promote lipid absorption in intestinal epithelial cells (21-23). The mRNA levels of jejunal *Cd36* were dramatically lower in $CT\alpha^{IKO}$ mice relative to control mice (Fig. 6F). Furthermore, *Slc27a4* and *Npc1l1* mRNA levels were modestly lower in $CT\alpha^{IKO}$ mice (Fig. 5F). Therefore, reduced expression of membrane transporters involved in intestinal lipid uptake relative to controls may at least partially account for impaired lipid absorption in $CT\alpha^{IKO}$ mice.

Loss of intestinal $CT\alpha$ enhances postprandial enteroendocrine hormone secretion

Dietary fatty acids in the lumen of the distal intestine stimulate secretion of enteroendocrine hormones including glucagon-like peptide 1 (GLP-1) and peptide YY (PYY) from L cells to control food intake and satiety (24). Since $CT\alpha^{IKO}$ mice have impaired fatty acid absorption in the proximal small intestine resulting in increased fatty acid content of feces, we hypothesized that the higher abundance of fatty acids in the distal small intestine of $CT\alpha^{IKO}$ mice would trigger GLP-1 and PYY secretion. $CT\alpha^{IKO}$ mice had strikingly elevated active GLP-1 (~9-fold) and PYY (~9-fold) in plasma 2 h after re-feeding the HFD (Fig. 7A and 7B). A major physiological function of GLP-1 is to promote insulin secretion from the pancreas (24). Accordingly, $CT\alpha^{IKO}$ mice had a strong trend towards higher postprandial plasma insulin concentrations compared to controls (Fig. 7C). Fibroblast-like growth factor 21 (FGF21) is a hepatokine with multiple systemic effects on carbohydrate and lipid metabolism and is highly responsive to changes in nutrient intake (25-27). Circulating concentrations of FGF21 were 4.5-fold higher in $CT\alpha^{IKO}$ mice compared to controls after HFD re-feeding (Fig. 7D). To test whether the observed changes to circulating hormone concentrations altered postprandial glucose

metabolism, we re-fed mice a HFD for 2 h before administering them with an oral glucose challenge. $CT\alpha^{IKO}$ mice had significantly lower peak blood glucose concentrations compared to controls after the glucose challenge (Fig. 7E). Importantly, re-fed plasma TG and GLP-1 were not different between tamoxifen-treated floxed controls and mice with a heterozygous deletion of intestinal $CT\alpha$ (Supplementary Fig.S1N and S1O). These data link impaired lipid uptake in the absence of intestinal $CT\alpha$ to enhanced postprandial enteric and hepatic hormone secretion, likely contributing to reduced body weight in $CT\alpha^{IKO}$ mice relative to control mice.

Loss of intestinal $CT\alpha$ alters enterohepatic circulation of bile acids and increases biliary PC secretion into the intestinal lumen

We were initially surprised that $CT\alpha^{IKO}$ mice can maintain epithelial cell turnover and intestinal viability in the absence of *de novo* PC synthesis. Thus, we hypothesized that increased biliary PC secretion may contribute to the maintenance of intestinal PC concentrations and intestinal epithelial cell viability in $CT\alpha^{IKO}$ mice. To examine biliary lipid and bile acid secretion, we cannulated the gallbladders of mice fed the HFD. The rate of bile flow in $CT\alpha^{IKO}$ mice was strikingly higher (~25%) than in control mice (Fig. 8A), coinciding with a doubling of biliary bile acid secretion, a 1.5-fold increase in phospholipid secretion and a 1.3-fold increase in cholesterol secretion (Fig. 8B-8D). Consistent with increased biliary lyso-PC delivery to the intestinal epithelium, the mRNA levels of jejunal *Lpcat4*, which catalyzes the addition of oleic acid to lyso-PC (28), was significantly higher in $CT\alpha^{IKO}$ mice 2 h after HFD re-feeding (Fig. 8E). Therefore, a higher rate of delivery of biliary PC to the intestines of $CT\alpha^{IKO}$ mice may contribute to their capacity to maintain intestinal epithelial cell viability in the absence of *de novo* intestinal PC synthesis.

While total biliary bile acid concentrations were higher in $CT\alpha^{IKO}$ mice, the bile acid species composition was largely unaltered, except for taurodeoxycholic acid, which was reduced (Fig. 8F). Consequently, the bile acid hydrophobicity index was similar between control and $CT\alpha^{IKO}$ mice (Fig. 8G). Additionally, a non-significant trend towards higher plasma bile acid concentrations in $CT\alpha^{IKO}$ mice fed the HFD was observed (Fig. 8H). There was no change in the hepatic expression of genes involved in bile acid synthesis, and total fecal bile acid concentrations were not different between $CT\alpha^{IKO}$ mice and control mice fed the HFD (Fig. 8I and 8J). These data strongly indicate that enhanced biliary bile acid and lipid secretion in $CT\alpha^{IKO}$ mice is not driven by an increase in hepatic bile acid synthesis.

There was a robust increase in mRNA levels of the apical sodium-bile acid transporter, *solute carrier family 10 member 2* (*Slc10a2/Asbt*; mainly restricted to the ileum under normal conditions), in the jejunum of $CT\alpha^{IKO}$ mice (Fig. 8K). An increase in jejunal *Asbt* is predicted to increase bile acid absorption in the proximal small intestine and to accelerate enterohepatic cycling of bile acids (29). In line with increased *Asbt*-mediated bile acid uptake in the proximal small intestine, mRNA levels of the bile-acid transporter *Fabp6* had a strong tendency towards an increase in the jejunum of $CT\alpha^{IKO}$ mice compared to controls 2 h after re-feeding. Furthermore, ileal *Slc10a2*, *Fabp6* and *Slc51b* mRNA levels were not different, while ileal *Slc51a* were lower in $CT\alpha^{IKO}$ mice than in ileums from control mice. Thus, loss of intestinal $CT\alpha$ stimulates the secretion of bile acids and lipids from the liver by a mechanism that involves a shift in reabsorption of bile acids to the proximal small intestine to promote enterohepatic cycling.

DISCUSSION

In this study we show that intestinal PC synthesis *via* CT α plays a crucial role in coordinating the metabolic response of mice to HFD feeding. Our data suggest that the metabolic response to a HFD in CT α^{IKO} mice is driven by a combination of impaired dietary lipid absorption, increased secretion of the fat-induced satiety hormones GLP-1 and PYY, and reduced food intake. Furthermore, a shift in expression of bile-acid responsive genes to the proximal small intestine of CT α^{IKO} mice is linked to accelerated enterohepatic bile acid cycling. Loss of intestinal CT α is not well tolerated by some mice fed a HFD, indicating that *de novo* PC synthesis is specifically required for normal intestinal metabolic function. Furthermore, our data show that re-acylation of lyso-PC from the intestinal lumen cannot compensate for loss of CT α -derived PC in enterocytes.

Mice with intestinal deletion of the gene encoding the PC remodeling enzyme *Lpcat3* have reduced chylomicron secretion when fed a chow diet due to failure to incorporate polyunsaturated fatty acids into intestinal PC, which alters membrane dynamics and fatty acid uptake (9, 10). In contrast, we found that *de novo* PC synthesis is not required for chylomicron secretion in the setting of a low-fat diet. This observation suggests that the re-acylation of lyso-PC derived from bile can fully accommodate chylomicron assembly under these conditions. However, an increase in cellular fatty acid concentrations increases cellular demand for PC to maintain membrane lipid homeostasis and produce the surface monolayer for lipid droplets and lipoproteins (2). Accordingly, HFD-fed CT α^{IKO} mice have disrupted intestinal metabolic function (likely due to constant influx of fatty acids into intestinal epithelial cells which increases cellular PC demands) including impaired dietary lipid uptake (despite minimal changes to the relative abundance of polyunsaturated PC species or *Lpcat3* expression in the intestine).

Therefore, both pathways for intestinal PC formation (i.e. *de novo* PC synthesis and PC remodeling) are independently required for dietary lipid absorption when consuming a HFD. Furthermore, *Lpcat3*-deficient mice do not experience changes in bile acid concentrations (10), suggesting that the pathways of *de novo* PC synthesis and PC remodeling also control distinct aspects of enterohepatic physiology.

We used a radiolabeled tracer to demonstrate that $CT\alpha^{IKO}$ mice fed a HFD have impaired jejunal fatty acid uptake, resulting in the production of chylomicrons with lower TG content. Impaired lipid uptake in mice lacking intestinal *de novo* PC synthesis is not due to gross damage to the intestinal epithelium, as electron microscopy revealed an intact brush border membrane. Instead, loss of intestinal $CT\alpha$ is linked to intestinal metabolic dysfunction in the setting of a HFD including reduced expression of genes involved in dietary lipid absorption. Targeted deletion of *Mogat2* (13), *Cd36* (21), *Abhd5* (30) and *Npc1l1* (23), all of which are lower in the intestines of $CT\alpha^{IKO}$ mice relative to controls, impairs dietary lipid absorption. Therefore, intestinal *de novo* PC synthesis apparently maintains a network of genes involved in dietary lipid uptake.

The intestinal epithelium is highly active in cell division, growth, differentiation, and secretion i.e. processes that require adequate PC supply (2). Therefore, we were surprised that $CT\alpha^{IKO}$ mice can maintain epithelial cell turnover and intestinal viability in the absence of *de novo* intestinal PC synthesis. Nevertheless, increased biliary PC secretion may contribute to the maintenance of intestinal PC concentrations in $CT\alpha^{IKO}$ mice. We unexpectedly found that deletion of intestinal $CT\alpha$ doubles the rate of biliary bile acid secretion in $CT\alpha^{IKO}$ mice compared to control mice. Because bile acids drive bile flow as well as biliary cholesterol and phospholipid secretion, these parameters were also significantly higher in $CT\alpha^{IKO}$ mice (31). The higher rate of

delivery of bile acids (with similar composition to bile acids in controls) into the intestinal lumen of $CT\alpha^{IKO}$ mice implies that impaired fatty acid absorption with loss of intestinal $CT\alpha$ is not due to a deficiency of mixed micelles required for efficient fat absorption. Furthermore, since the cholesterol labeling study, the analysis of fecal bile output, and measurement of expression of bile acid-synthetic genes revealed that hepatic bile acid synthesis is not induced by loss of intestinal $CT\alpha$, enterohepatic cycling of bile acids is likely accelerated. This hypothesis is supported by a shift in expression of *Slc10a2* and *Fabp6* towards more proximal parts of the small intestine. A shift in the expression of bile-acid responsive genes to the proximal intestine has been reported previously in mice lacking intestinal GATA4, a transcription factor that controls jejunal-ileal identity (32, 33). The change in spatial expression of bile-acid responsive genes in intestinal GATA4 deficient mice is also linked to impaired lipid absorption (33) and increased bile flow (29). Clearly, the molecular mechanisms that regulate crosstalk between the intestine and liver in controlling bile formation in $CT\alpha^{IKO}$ mice require further research. Changes to enterohepatic circulation of bile acids can influence lipid, carbohydrate, and energy metabolism (34). Furthermore, bile acids increase the circulating level of FGF21 (35), a hepatokine that is increased in $CT\alpha^{IKO}$ mice and that reduces adiposity when administered pharmacologically (25). Therefore, changes in bile acid metabolism may contribute to metabolic adaptations in the $CT\alpha^{IKO}$ mice fed a HFD.

GLP-1 and PYY are hormones that can influence energy balance through both the enteric nervous system and peripheral targets after nutrient-induced secretion from L cells (24). Under normal conditions, most dietary fatty acids are absorbed in the proximal small intestine (Fig. 4C). However, if high concentrations of fatty acids reach L cells of the distal intestine they can enhance GLP-1 and PYY secretion (24). Accordingly, mice with intestinal deletion of genes

involved in dietary fat absorption, including *Mogat2* (13), *Dgat1* (36) and *Lpcat3* (10), have relatively high postprandial plasma GLP-1 concentrations. Similarly, impaired HFD absorption in the proximal small intestine of $CT\alpha^{IKO}$ mice allows fatty acids to reach the distal intestine to potentiate enteroendocrine hormone secretion. The stimulation of GLP-1 and PYY secretion by fatty acids in $CT\alpha^{IKO}$ mice likely contributes to their relatively more severe response to a HFD compared to a chow diet, as was observed in intestine-specific *Lpcat3*-deficient mice (10). High postprandial plasma GLP-1 is associated with increased insulin secretion and lower blood glucose concentrations in $CT\alpha^{IKO}$ mice compared to control mice fed a HFD. Furthermore, enhanced GLP-1-mediated insulin secretion might account for the lower plasma free fatty acid concentrations in $CT\alpha^{IKO}$ mice compared to controls by suppressing lipolysis in adipocytes. Additionally, enhanced PYY secretion in $CT\alpha^{IKO}$ mice could contribute to their reduced body weight by interacting with brain regions that control energy balance (37). Taken together, our findings demonstrate that modulation of intestinal phospholipid metabolism can influence whole-body physiology by enhancing the secretion of metabolically active hormones.

In conclusion, this study demonstrates that intestinal *de novo* PC synthesis plays a central role in dietary lipid absorption during HFD feeding. Loss of intestinal $CT\alpha$ amplifies postprandial GLP-1 and PYY secretion and alters circulating glucose and free fatty acid concentrations, linking gut phospholipid synthesis to whole-body nutrient disposal and metabolism. Our studies also reveal an unexpected role for intestinal *de novo* PC synthesis in the maintenance of normal enterohepatic circulation of bile acids, potentially by governing the spatial expression of the bile-acid transporter *Slc10a2* in the intestine. Therefore, a physiologically normal response to dietary fat intake depends on *de novo* PC synthesis in the

intestinal epithelium, and the re-acylation of PC derived from extra-intestinal sources cannot fulfill this requirement.

ACKNOWLEDGEMENTS

The authors thank Dr. Patricia Brubacker for Villin-CreER^{T2} mice. We thank Nicole Coursen, Susanne Lingrell, Ying Wayne Wang, Rongjia Liu and Dr. Kunimasa Suzuki for technical assistance. We thank Audric Moses and the University of Alberta Lipidomics Core Facility. We thank Drs. Jean Vance, Dennis Vance, and Richard Lehner for critical evaluation of the manuscript, and Ms. Ruth Jacobs for critical editing of the grant. We thank Priscilla Guo and Dr. Xuejun Sun for assistance with electron microscopy, Amy Barr of the University of Alberta Cardiovascular Research Centre, and Lynette Elder of the Alberta Diabetes Institute Histology Core. This work was supported by grants from the Canadian Institutes of Health Research (to R.L.J), the Alberta Diabetes Institute (to R.L.J and J.P.K), and Alberta Innovates – Technology Futures (to J.P.K).

REFERENCES

1. van der Veen, J. N., J. P. Kennelly, S. Wan, J. E. Vance, D. E. Vance, and R. L. Jacobs. 2017. The critical role of phosphatidylcholine and phosphatidylethanolamine metabolism in health and disease. *Biochim Biophys Acta* **1859**: 1558-1572.
2. Cornell, R. B., and N. D. Ridgway. 2015. CTP:phosphocholine cytidyltransferase: Function, regulation, and structure of an amphitropic enzyme required for membrane biogenesis. *Prog Lipid Res* **59**: 147-171.
3. Wang, L., S. Magdaleno, I. Tabas, and S. Jackowski. 2005. Early embryonic lethality in mice with targeted deletion of the CTP:phosphocholine cytidyltransferase alpha gene (Pcvt1a). *Mol Cell Biol* **25**: 3357-3363.

4. Jacobs, R. L., C. Devlin, I. Tabas, and D. E. Vance. 2004. Targeted deletion of hepatic CTP:phosphocholine cytidyltransferase alpha in mice decreases plasma high density and very low density lipoproteins. *J Biol Chem* **279**: 47402-47410.
5. Noga, A. A., Y. Zhao, and D. E. Vance. 2002. An unexpected requirement for phosphatidylethanolamine N-methyltransferase in the secretion of very low density lipoproteins. *J Biol Chem* **277**: 42358-42365.
6. Nilsson, A. 1968. Intestinal absorption of lecithin and lysolecithin by lymph fistula rats. *Biochim Biophys Acta* **152**: 379-390.
7. Parthasarathy, S., P. V. Subbaiah, and J. Ganguly. 1974. The mechanism of intestinal absorption of phosphatidylcholine in rats. *Biochem J* **140**: 503-508.
8. Voshol, P. J., D. M. Minich, R. Havinga, R. P. Elferink, H. J. Verkade, A. K. Groen, and F. Kuipers. 2000. Postprandial chylomicron formation and fat absorption in multidrug resistance gene 2 P-glycoprotein-deficient mice. *Gastroenterology* **118**: 173-182.
9. Li, Z., H. Jiang, T. Ding, C. Lou, H. H. Bui, M. S. Kuo, and X. C. Jiang. 2015. Deficiency in lysophosphatidylcholine acyltransferase 3 reduces plasma levels of lipids by reducing lipid absorption in mice. *Gastroenterology* **149**: 1519-1529.
10. Wang, B., X. Rong, M. A. Duerr, D. J. Hermanson, P. N. Hedde, J. S. Wong, T. Q. Vallim, B. F. Cravatt, E. Gratton, D. A. Ford, and P. Tontonoz. 2016. Intestinal Phospholipid Remodeling Is Required for Dietary-Lipid Uptake and Survival on a High-Fat Diet. *Cell Metab* **23**: 492-504.
11. Tso, P., H. Kendrick, J. A. Balint, and W. J. Simmonds. 1981. Role of biliary phosphatidylcholine in the absorption and transport of dietary triolein in the rat. *Gastroenterology* **80**: 60-65.
12. el Marjou, F., K. P. Janssen, B. H. Chang, M. Li, V. Hindie, L. Chan, D. Louvard, P. Chambon, D. Metzger, and S. Robine. 2004. Tissue-specific and inducible Cre-mediated recombination in the gut epithelium. *Genesis* **39**: 186-193.
13. Yen, C. L., M. L. Cheong, C. Grueter, P. Zhou, J. Moriwaki, J. S. Wong, B. Hubbard, S. Marmor, and R. V. Farese. 2009. Deficiency of the intestinal enzyme acyl CoA:monoacylglycerol acyltransferase-2 protects mice from metabolic disorders induced by high-fat feeding. *Nat Med* **15**: 442-446.
14. FOLCH, J., M. LEES, and G. H. SLOANE STANLEY. 1957. A simple method for the isolation and purification of total lipides from animal tissues. *J Biol Chem* **226**: 497-509.
15. Alnouti, Y., I. L. Csanaky, and C. D. Klaassen. 2008. Quantitative-profiling of bile acids and their conjugates in mouse liver, bile, plasma, and urine using LC-MS/MS. *J Chromatogr B Analyt Technol Biomed Life Sci* **873**: 209-217.
16. Heuman, D. M. 1989. Quantitative estimation of the hydrophilic-hydrophobic balance of mixed bile salt solutions. *J Lipid Res* **30**: 719-730.
17. Zhou, X., and G. Arthur. 1992. Improved procedures for the determination of lipid phosphorus by malachite green. *J Lipid Res* **33**: 1233-1236.
18. Mashige, F., K. Imai, and T. Osuga. 1976. A simple and sensitive assay of total serum bile acids. *Clin Chim Acta* **70**: 79-86.
19. Myher, J. J., and A. Kuksis. 1984. Determination of plasma total lipid profiles by capillary gas-liquid chromatography. *J Biochem Biophys Methods* **10**: 13-23.
20. Wang, B., X. Rong, E. N. D. Palladino, J. Wang, A. M. Fogelman, M. G. Martín, W. A. Alrefai, D. A. Ford, and P. Tontonoz. 2018. Phospholipid Remodeling and Cholesterol Availability Regulate Intestinal Stemness and Tumorigenesis. *Cell Stem Cell* **22**: 206-220.e204.

21. Drover, V. A., M. Ajmal, F. Nassir, N. O. Davidson, A. M. Nauli, D. Sahoo, P. Tso, and N. A. Abumrad. 2005. CD36 deficiency impairs intestinal lipid secretion and clearance of chylomicrons from the blood. *J Clin Invest* **115**: 1290-1297.
22. Stahl, A., D. J. Hirsch, R. E. Gimeno, S. Punreddy, P. Ge, N. Watson, S. Patel, M. Kotler, A. Raimondi, L. A. Tartaglia, and H. F. Lodish. 1999. Identification of the major intestinal fatty acid transport protein. *Mol Cell* **4**: 299-308.
23. Altmann, S. W., H. R. Davis, L. J. Zhu, X. Yao, L. M. Hoos, G. Tetzloff, S. P. Iyer, M. Maguire, A. Golovko, M. Zeng, L. Wang, N. Murgolo, and M. P. Graziano. 2004. Niemann-Pick C1 Like 1 protein is critical for intestinal cholesterol absorption. *Science* **303**: 1201-1204.
24. Cummings, D. E., and J. Overduin. 2007. Gastrointestinal regulation of food intake. *J Clin Invest* **117**: 13-23.
25. Fisher, F. M., and E. Maratos-Flier. 2016. Understanding the Physiology of FGF21. *Annu Rev Physiol* **78**: 223-241.
26. Badman, M. K., P. Pissios, A. R. Kennedy, G. Koukos, J. S. Flier, and E. Maratos-Flier. 2007. Hepatic fibroblast growth factor 21 is regulated by PPARalpha and is a key mediator of hepatic lipid metabolism in ketotic states. *Cell Metab* **5**: 426-437.
27. Kharitonov, A., T. L. Shiyanova, A. Koester, A. M. Ford, R. Micanovic, E. J. Galbreath, G. E. Sandusky, L. J. Hammond, J. S. Moyers, R. A. Owens, J. Gromada, J. T. Brozinick, E. D. Hawkins, V. J. Wroblewski, D. S. Li, F. Mehrbod, S. R. Jaskunas, and A. B. Shanafelt. 2005. FGF-21 as a novel metabolic regulator. *J Clin Invest* **115**: 1627-1635.
28. Hishikawa, D., H. Shindou, S. Kobayashi, H. Nakanishi, R. Taguchi, and T. Shimizu. 2008. Discovery of a lysophospholipid acyltransferase family essential for membrane asymmetry and diversity. *Proc Natl Acad Sci U S A* **105**: 2830-2835.
29. Out, C., J. V. Patankar, M. Doktorova, M. Boesjes, T. Bos, S. de Boer, R. Havinga, H. Wolters, R. Boverhof, T. H. van Dijk, A. Smoczek, A. Bleich, V. Sachdev, D. Kratky, F. Kuipers, H. J. Verkade, and A. K. Groen. 2015. Gut microbiota inhibit Asbt-dependent intestinal bile acid reabsorption via Gata4. *J Hepatol* **63**: 697-704.
30. Xie, P., F. Guo, Y. Ma, H. Zhu, F. Wang, B. Xue, H. Shi, J. Yang, and L. Yu. 2014. Intestinal Cgi-58 deficiency reduces postprandial lipid absorption. *PLoS One* **9**: e91652.
31. Verkade, H. J., R. J. Vonk, and F. Kuipers. 1995. New insights into the mechanism of bile acid-induced biliary lipid secretion. *Hepatology* **21**: 1174-1189.
32. Bosse, T., C. M. Piaseckyj, E. Burghard, J. J. Fialkovich, S. Rajagopal, W. T. Pu, and S. D. Krasinski. 2006. Gata4 is essential for the maintenance of jejunal-ileal identities in the adult mouse small intestine. *Mol Cell Biol* **26**: 9060-9070.
33. Battle, M. A., B. J. Bondow, M. A. Iverson, S. J. Adams, R. J. Jandacek, P. Tso, and S. A. Duncan. 2008. GATA4 is essential for jejunal function in mice. *Gastroenterology* **135**: 1676-1686.e1671.
34. Cariou, B., K. van Harmelen, D. Duran-Sandoval, T. H. van Dijk, A. Grefhorst, M. Abdelkarim, S. Caron, G. Torpier, J. C. Fruchart, F. J. Gonzalez, F. Kuipers, and B. Staels. 2006. The farnesoid X receptor modulates adiposity and peripheral insulin sensitivity in mice. *J Biol Chem* **281**: 11039-11049.
35. Cyphert, H. A., X. Ge, A. B. Kohan, L. M. Salati, Y. Zhang, and F. B. Hillgartner. 2012. Activation of the farnesoid X receptor induces hepatic expression and secretion of fibroblast growth factor 21. *J Biol Chem* **287**: 25123-25138.
36. Ables, G. P., K. J. Yang, S. Vogel, A. Hernandez-Ono, S. Yu, J. J. Yuen, S. Birtles, L. K. Buckett, A. V. Turnbull, I. J. Goldberg, W. S. Blaner, L. S. Huang, and H. N. Ginsberg. 2012.

Intestinal DGAT1 deficiency reduces postprandial triglyceride and retinyl ester excursions by inhibiting chylomicron secretion and delaying gastric emptying. *J Lipid Res* **53**: 2364-2379.

37. Stadlbauer, U., M. Arnold, E. Weber, and W. Langhans. 2013. Possible mechanisms of circulating PYY-induced satiation in male rats. *Endocrinology* **154**: 193-204.

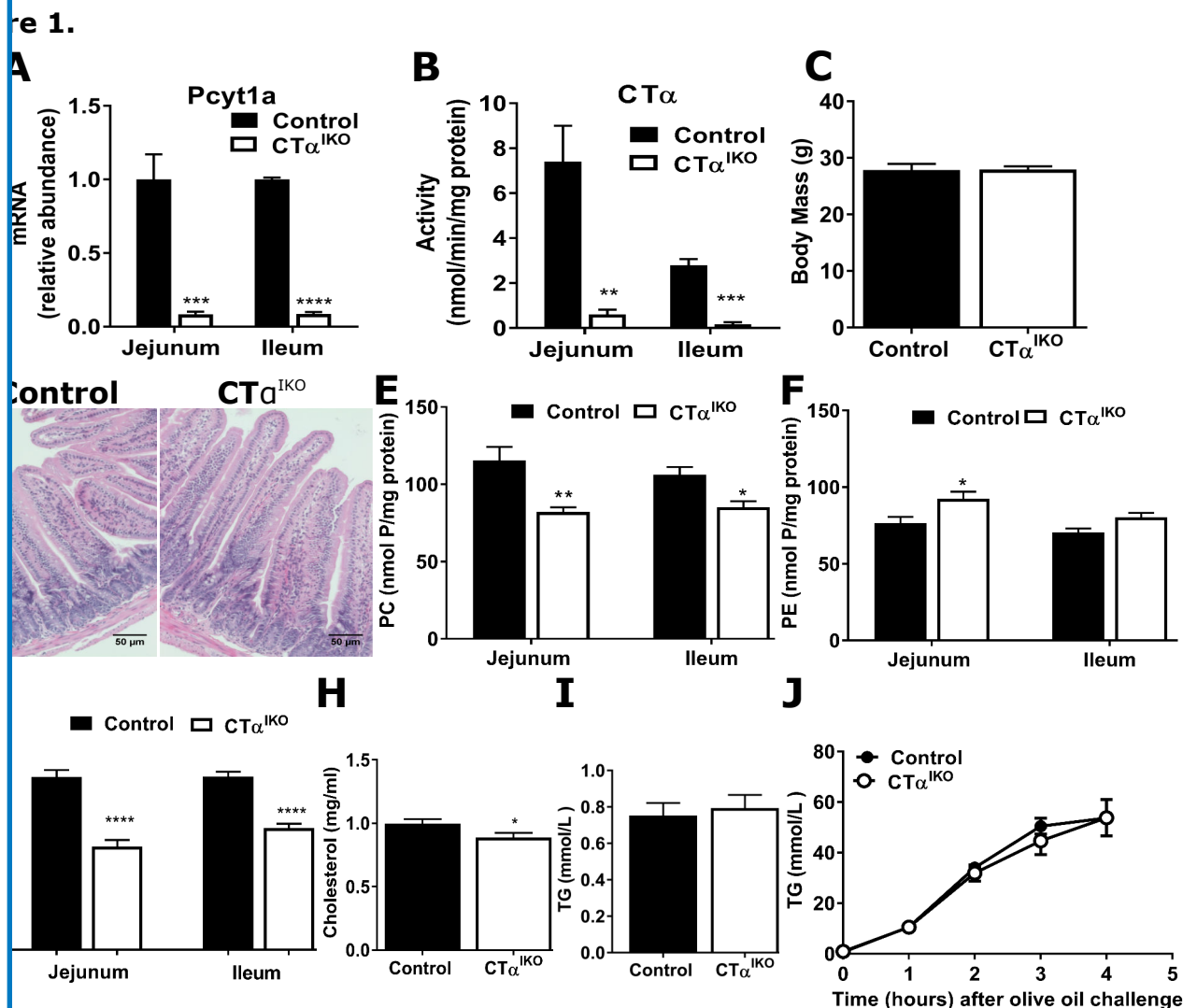
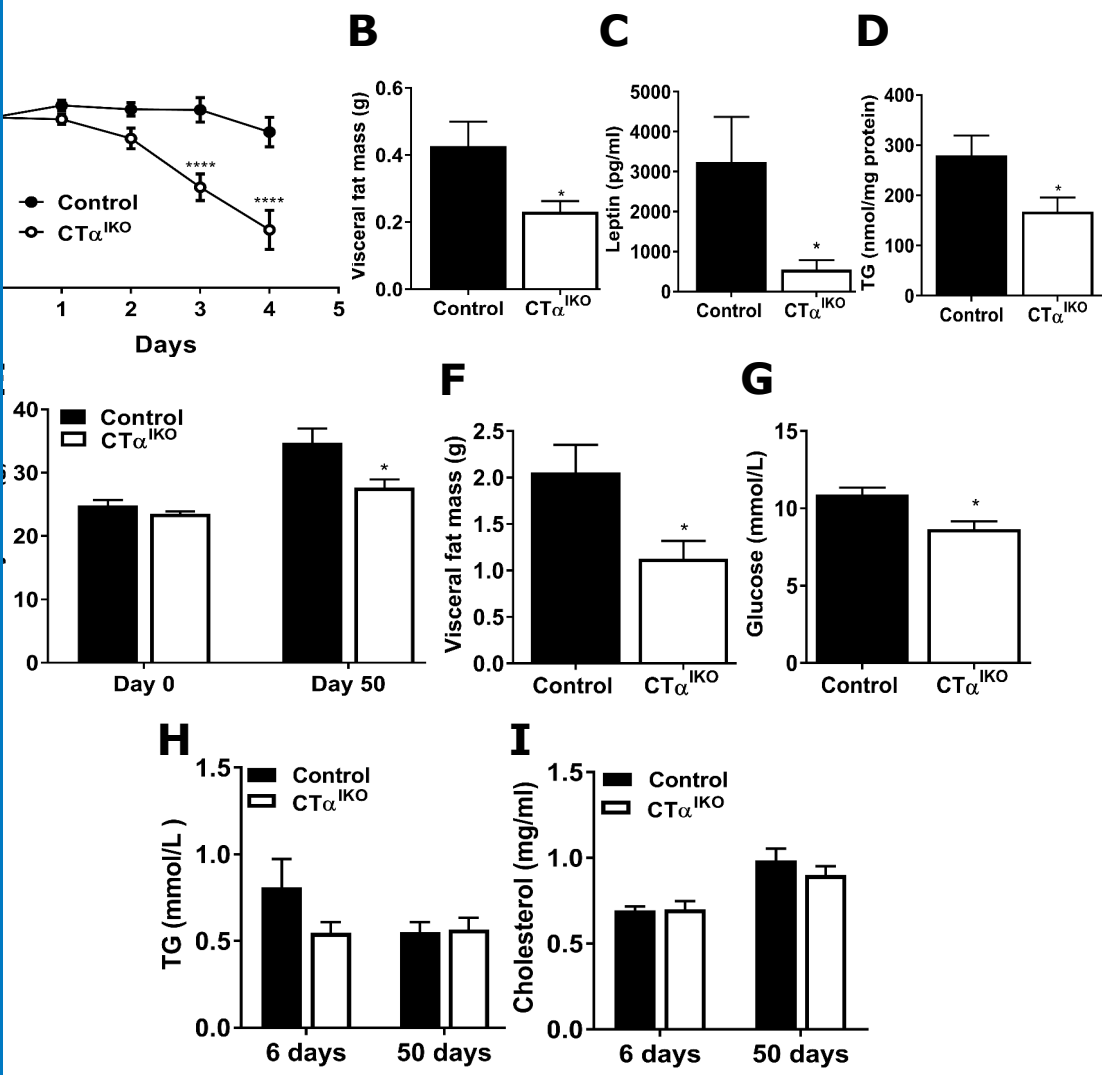


Fig. 1. Intestinal PC concentrations are reduced in CT α^{IKO} mice fed a chow diet, but fat absorption capacity is unaltered. (A) *Pcyt1a* mRNA abundance, and (B) CT α enzyme activity in the jejunum and ileum of control and CT α^{IKO} mice 5 days after Cre induction. Male control and CT α^{IKO} mice were fed chow diet for 6 weeks following Cre induction before being fasted for 10h, intraperitoneally injected with floxamer-407, and gavaged with olive oil. (C) Fasting body mass of male control mice and CT α^{IKO} mice fed the chow diet for 6 weeks (n=10-11/group). (D) Representative H&E stained jejunum sections from control mice and CT α^{IKO} mice fed the chow diet for 6 weeks. (E) PC concentrations in the jejunum and ileum (n=5/group). (F) PE concentrations in the jejunum and ileum (n=5/group). (G) Molar ratio of PC-to-PE in the jejunum and ileum (n=5/group). (H) Fasting plasma cholesterol, (I) fasting plasma TG, and (J) Plasma TG before and 1, 2, 3, 4 h following the oral bolus of olive oil in mice fed the chow diet for 6 weeks. Values are means \pm SEM, n=5/group. *p<.05, **p<.01, ***p<.001, ****p<.0001.

re 2.



HFD feeding initially induces rapid weight loss, while chronic HFD feeding reduces weight gain, in CT α ^{IKO} mice. (A) Body mass change relative to total body mass at time of initiation of the HFD; graph is representative of 2 independent experiments (n=5/group). (B) Visceral fat mass, (C) plasma leptin concentrations, (D) liver TG of control and CT α ^{IKO} mice on day 6 following initiation of the HFD (n=6/group). (E) Body mass of control mice and CT α ^{IKO} mice on day 0 and day 50 after initiation of the HFD (n=5/group). (F) Visceral fat mass, and (G) blood glucose concentrations of control mice and CT α ^{IKO} mice on day 50 after initiation of the HFD (n=5/group). (H) Fasting plasma TG, and (I) fasting plasma cholesterol concentrations of control mice and CT α ^{IKO} mice on day 6 and day 50 after initiation of the HFD (n \geq 5/group). All mice were female. Data are means \pm SEM. *p<.05, ****p<.0001.

Figure 3.

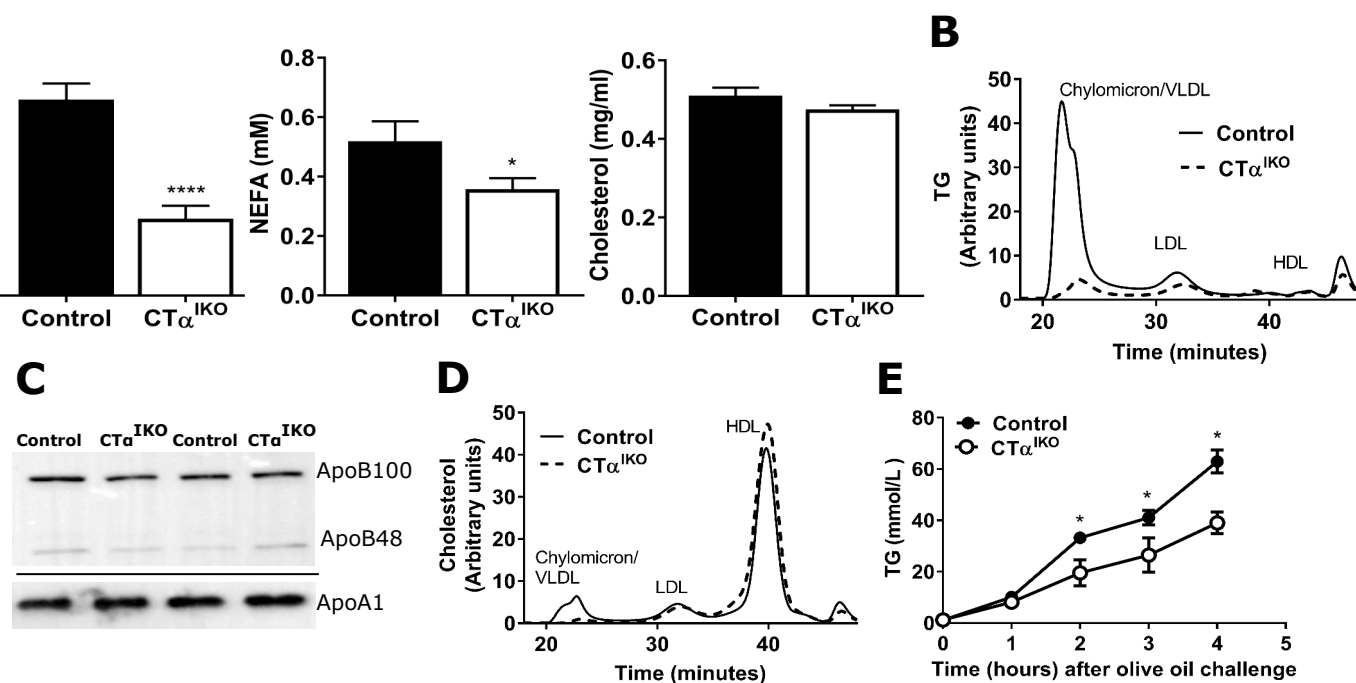


Fig. 3. CT α ^{IKO} mice fed a HFD have impaired intestinal TG secretion after a meal. Control and CT α ^{IKO} mice were fasted overnight and re-fed the HFD for 2 h. (A) Plasma TG, non-esterified fatty acids, and cholesterol after re-feeding (n=10/group). (B) FPLC of plasma lipoprotein TG after re-feeding (pooled plasma samples from n=5/group). (C) Representative immunoblot of plasma apolipoproteins after re-feeding (ApoB and ApoA1 were run on separate gels). (D) FPLC of plasma lipoprotein cholesterol after re-feeding (pooled plasma samples from n=5/group). (E) Plasma TG before and 1, 2, 3, 4 h following an oral bolus of olive oil and intraperitoneal injection of Poloxamer-407. (n=4/group). All mice were female. Values are means \pm SEM. *p<.05, ****p<.0001.

Figure 4.

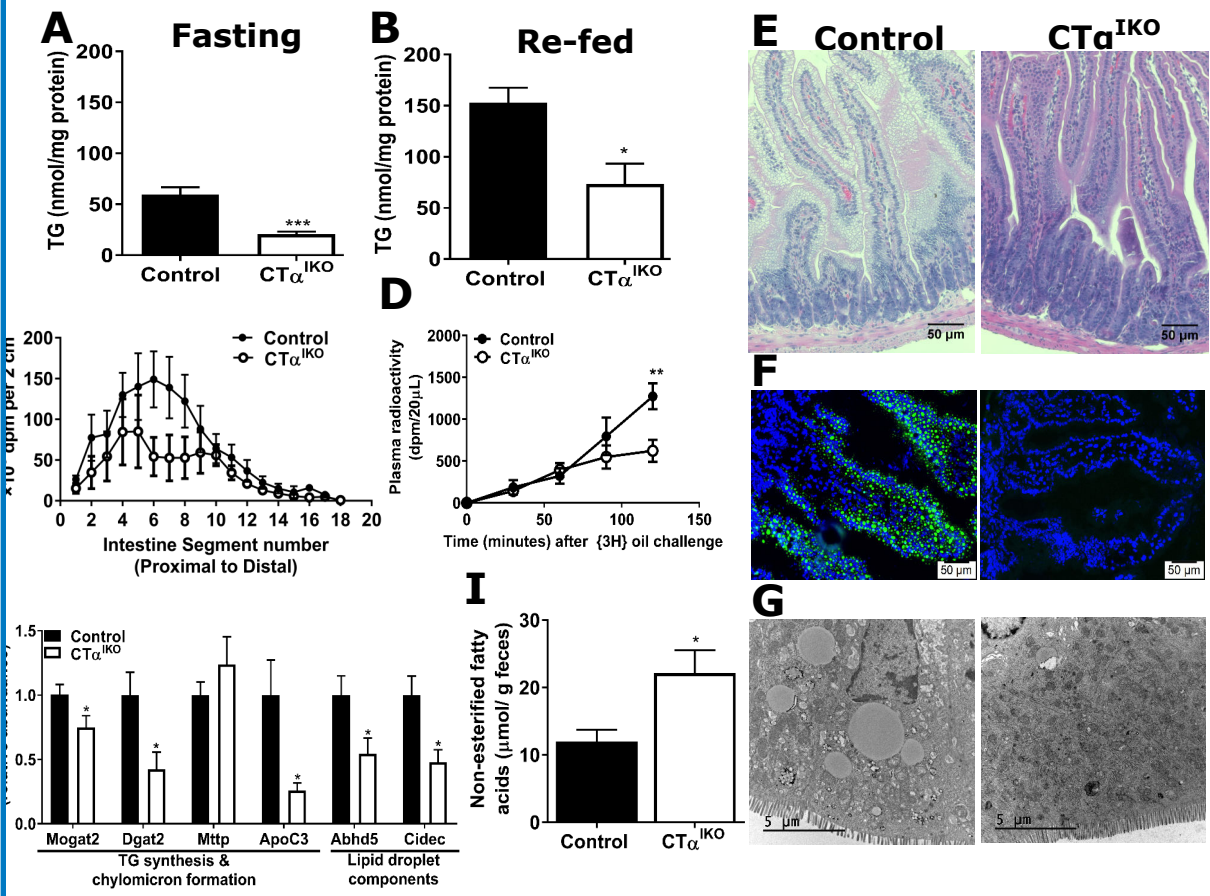
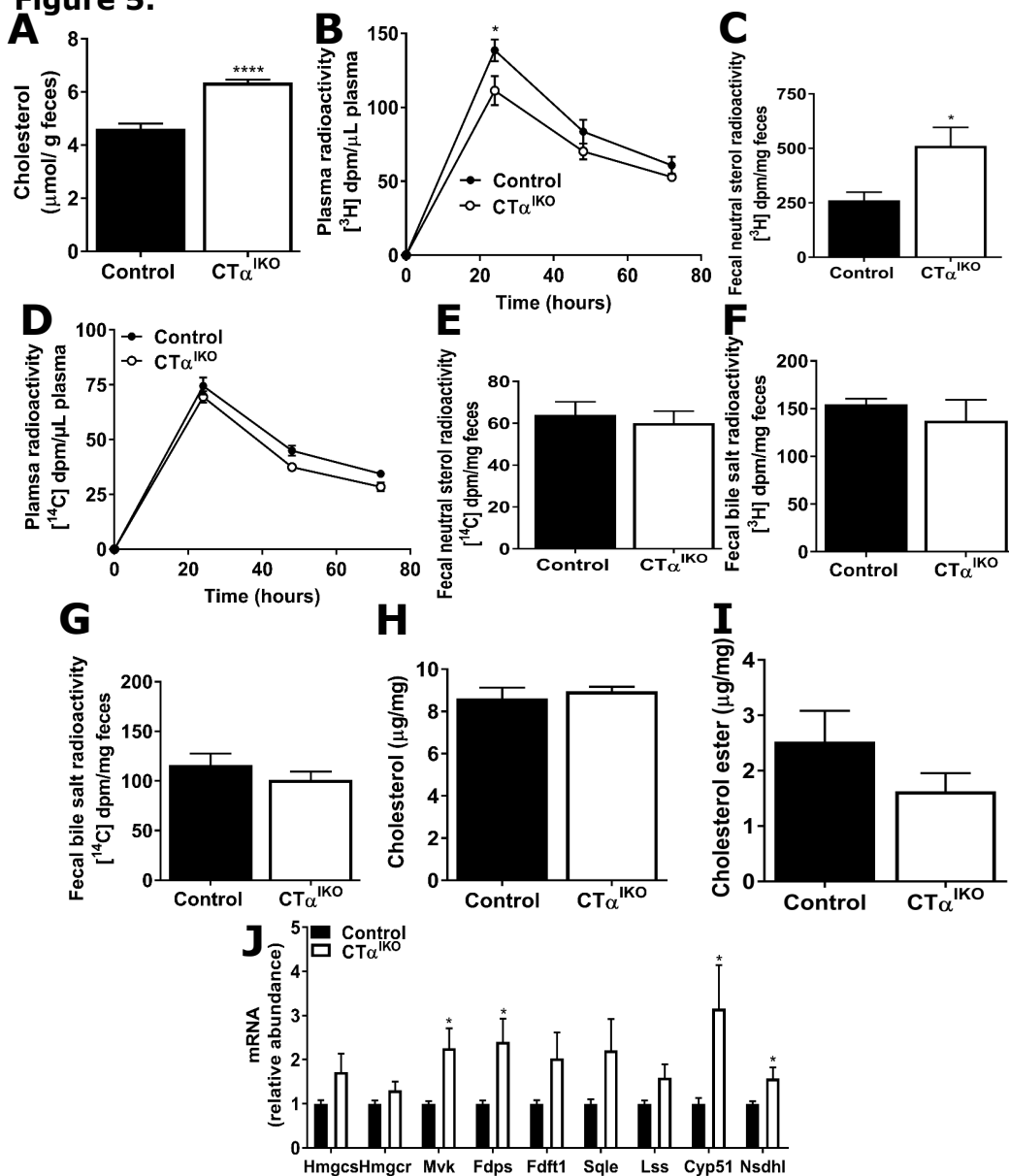


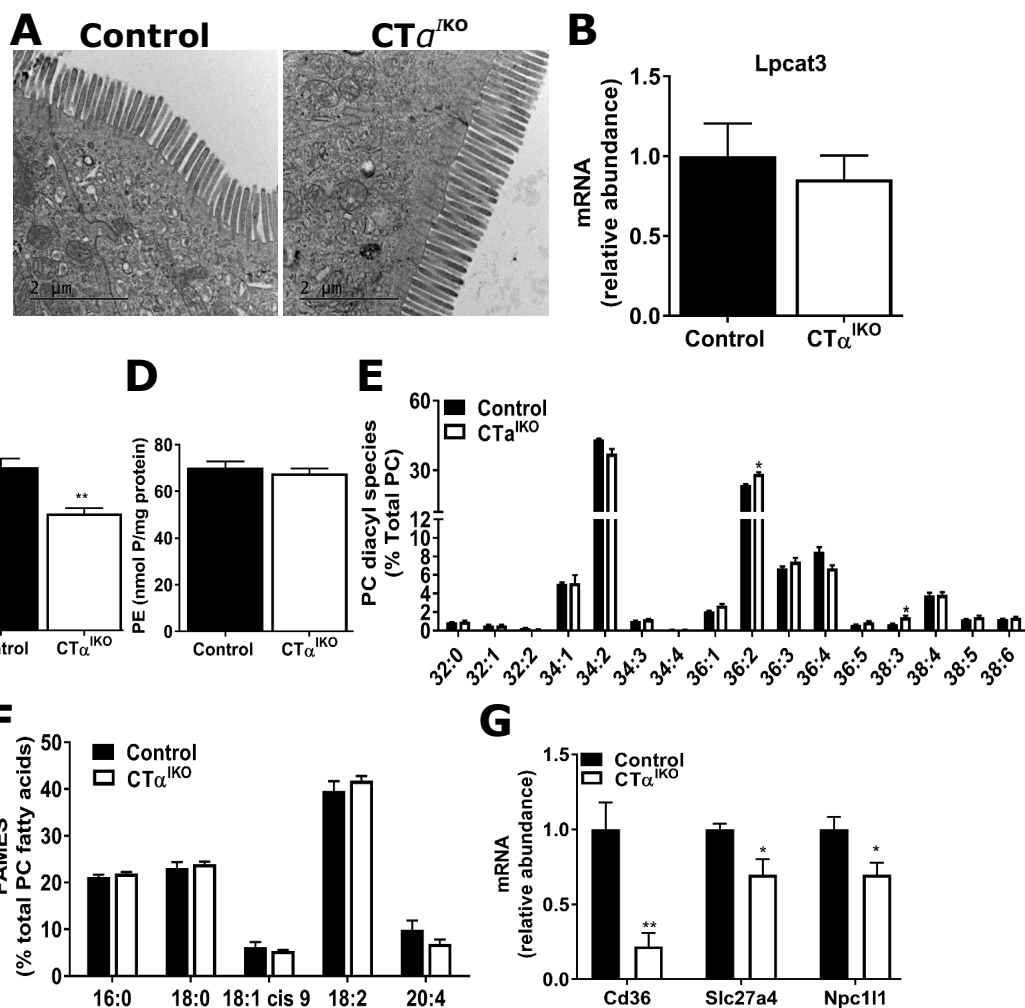
Fig.4. CT α ^{KO} mice fed a HFD have impaired passage of fatty acids from the intestinal lumen into enterocytes. Jejunal TG concentrations of female control and CT α ^{KO} mice after (A) fasting or (B) 2h after re-feeding the HFD (n=5-6/group). Male control and CT α ^{KO} mice were fasted for 4 h on day 3 following initiation of the HFD before receiving an oral bolus of 5 μ Ci [³H]-labeled triolein in 150 μ L olive oil for 2h (n=5/group). (C) Radiolabel in intestine segments 2 h after [³H]-labeled triolein gavage. (D) Plasma radiolabel before and 30, 60, 90 and 120 mins after a [³H]-labeled triolein gavage. Female control and CT α ^{KO} mice were fasted for 4 h on day 3 following initiation of the HFD before receiving an oral bolus of Bodipy-labelled olive oil. (E) Representative H&E stained proximal intestine sections of control and CT α ^{KO} mice 2 h after oil gavage. (F) Fluorescence microscope images of jejunal sections 2 h after Bodipy-labeled oil gavage. (G) Representative Transmission Electron Micrographs of jejunal enterocytes 2 h after oil gavage. (H) Jejunal mRNA abundance of genes involved in chylomicron and lipid droplet formation (n \geq 5/group). (I) Fatty acids in fecal samples from female control and CT α ^{KO} mice (n=5/group). Values are means \pm SEM. *p<.05, **p<.01, ***p<.001

Figure 5.



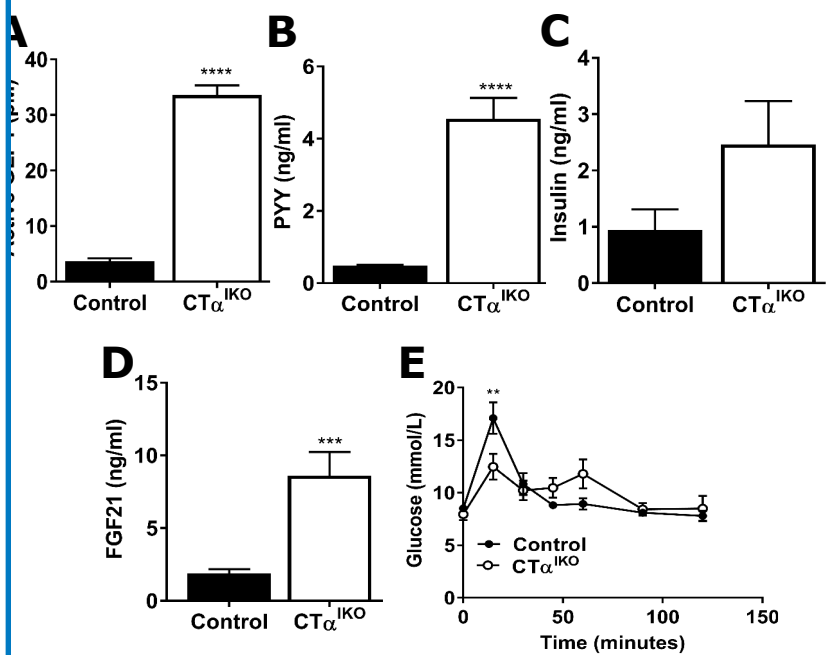
g. 5. Loss of intestinal CT α reduces dietary cholesterol absorption. (A) Cholesterol in fecal samples from female control and CT α^{IKO} mice (n=5/group). Male control and CT α^{IKO} received an oral dose of [^3H]-cholesterol (2 μCi) with 6mg unlabeled cholesterol in 150 μL of olive oil, and an intravenous injection of [^{14}C]-cholesterol (1 μCi) mixed in Intralipid®. Blood and feces were collected at 24, 48 and 72 h after cholesterol administration (n=4/group). (B) Plasma [^3H]-label at 24, 48 and 72 h. (C) Cumulative counts in fecal [^3H]-labelled neutral sterols over 72 h. (D) Plasma [^{14}C]-label at 24, 48 and 72 h. (E) Cumulative counts in fecal [^{14}C]-labelled neutral sterols over 72 h. (F) Cumulative [^3H]-label in bile salts, and (G) cumulative [^{14}C]-label in bile salt over 72 h. (H) non-esterified cholesterol, (I) cholesterol esters, and (J) mRNA abundance of cholesterol synthetic genes in the jejunum of control mice and CT α^{IKO} mice re-fed the HFD (n=4-5/group). Values are means \pm SEM. *p<.05, ****p<.0001.

Figure 6.



6. CT α ^{IKO} mice do not have damage to the brush border membrane or changes to the relative abundance of jejunal PC molecular species but do have reduced jejunal expression of genes encoding proteins involved in lipid uptake. (A) Representative Transmission Electron Micrographs of intestinal microvilli of control and CT α ^{IKO} mice fed the HFD. (B) *Lpcat3* mRNA abundance in the jejunum of control and CT α ^{IKO} mice (n=5/group). (C) PE concentrations in the jejunum of control and CT α ^{IKO} mice 2 h after HFD re-feeding (n=5/group). (D) The relative abundance of jejunal PC molecular species, (E) fatty acid methyl esters in PC of control mice and CT α ^{IKO} mice re-fed the HFD 2 h (n=4-5/group) (F) mRNA abundance of *Cd36*, *Slc27a4* and *Npc111* in the jejunum of control and CT α ^{IKO} mice 2 h after HFD re-feeding (n≥4/group). All mice were female. Values are means ± SEM. *p<.05, **p<.01

Figure 7.



7. CT α ^{IKO} mice have enhanced GLP-1, PYY and FGF21 secretion after a high-fat meal. Control and CT α ^{IKO} mice were fasted overnight on day 3 following initiation of the HFD before being re-fed for 2 h. (A) Plasma active GLP-1 (n=5/group). (B) Plasma PYY (n=10/group). (C) Plasma insulin (n=10/group). (D) Plasma FGF21 (n=10/group). (E) Blood glucose concentrations in control and CT α ^{IKO} mice re-fed the HFD for 2 h followed by an oral bolus of glucose. All mice were female. Values are means \pm SEM. *p<.05, **p<.01, ***p<.001, ****p<.0001.

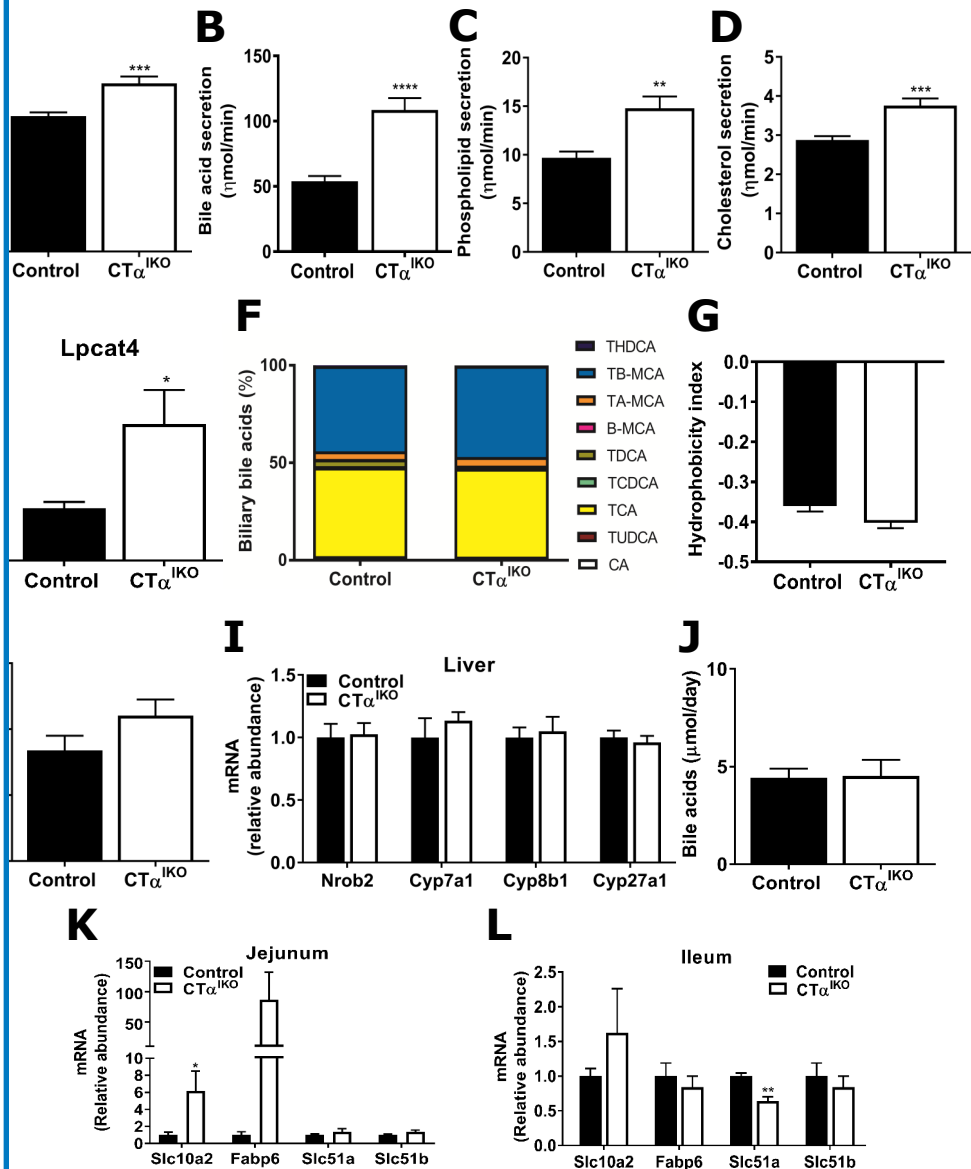


Fig. 8. Loss of intestinal CT α enhances biliary bile acid secretion. Gallbladders of male control and CT α^{IKO} mice were cannulated and bile was collected in pre-weighed containers (n=6-8/group). (A) Bile flow. (B) Bile salt secretion. (C) Phospholipid secretion. (D) Cholesterol secretion. (E) Jejunal *Lpcat4* expression. (F) Relative biliary bile acid composition. (G) bile acid hydrophobicity index. (H) Plasma bile acids. (I) mRNA abundance of hepatic genes involved in bile acid synthesis. (J) Fecal bile acids. (K) mRNA abundance of jejunal bile-acid responsive genes (n \geq 4/group), and (L) mRNA abundance of ileal bile-acid responsive genes in control mice and CT α^{IKO} mice 2 h after re-feeding the HFD (n=3/group). Values are means \pm SEM. *p<.05, **p<.01, ***p<.001, ****p<.0001.